How to walk carrying a huge egg? Trade-offs between locomotion and reproduction explain the special pelvis and leg anatomy in kiwi (Aves; Apteryx spp.)

Anick Abourachid, Isabel Castro, Pauline Provini

Title: How to walk with a huge egg? Trade-offs between locomotion and reproduction explain the special pelvis and leg anatomy in kiwi (Aves; *Apteryx* spp.)

Short running page heading: How to walk with a huge egg?

Authors: Anick Abourachid[1], Isabel Castro[2], Pauline Provini[1]

Affiliations:
[1] Département Adaptations du Vivant, UMR Mécanismes adaptatifs et évolution (MECADEV) Muséum National d'Histoire Naturelle / CNRS, 57 rue Cuvier, Case Postale 55, 75231 Paris Cedex 05, France.
[2] Wildlife and Ecology Group, Massey University, Private Bag 11222, Palmerston North 4410, New Zealand

Correspondence to:
Pauline Provini
Département Adaptations du Vivant
UMR Mécanismes adaptatifs et évolution (MECADEV), Muséum National D'Histoire Naturelle / CNRS
55 rue Buffon Case postale 55
75005 Paris Cedex 5 France
E-mail: Pauline.provini@mnhn.fr
Phone: +33 140793286

Abstract

Kiwi (Aves; genus *Apteryx*) are famous for laying an enormous egg in comparison to their relatively small body size. Considering the peculiar gait of this flightless bird, we suspected the existence of morpho-functional trade-offs between reproduction and locomotion. To understand how structural constraints, imposed by a large egg size, might influence the terrestrial locomotion of *Apteryx*, we analysed the anatomy of the limb osteo-muscular system in two species of kiwi (*Apteryx mantelli* and *Apteryx owenii*). We performed detailed dissections and brought to light specific anatomical features of kiwi, in comparison with other ratites and neognathous birds. Our osteological study revealed a strongly curved pelvis, a rigid tail, and enlarged ribs. Our myology study showed an unusual location of the *caudofemoralis* muscle origin and insertion. The insertion of the *pars pelvica* along the entire caudal face of the femur, contrasts with the proximal insertion usually seen in other birds. Additionally, the *pars caudalis* originates along the entire tail, whereas it only inserts on the uropygium in the other birds. To interpret these specificities from a functional point of view, we built three-dimensional osteomuscular models based on CT-scans, radiographies, and our dissections. We chose three postures associated with reproductive constraints: the standing position of a gravid compared to a non-gravid bird, as well as the brooding position. The 3D model of the brooding position suggested that the enlarged ribs could support the body weight when leaning on the huge egg in both male and female. Moreover, we found that in gravid females, the unusual shape of the pelvis and tail allowed the huge egg to sit ventrally below the pelvis, whereas it is held closer to the rachis in other birds. The specific conformation of the limb and the insertions of the two parses of the *caudofemoralis* help to maintain the tail flexed, and to keep the legs adducted when carrying the egg. The caudal location of the hip and its flexed position explains the long stance phase during the strange gait of kiwi, revealing the functional trade-off between reproduction and locomotion in this emblematic New Zealand bird.

Keywords:

New Zealand, gravid, egg incubation, hind limb, lower appendicular skeleton, myology, osteology, bird morphology.

Introduction

Kiwi (Aves; genus *Apteryx*; five species) are outlandish, in many aspects of their biology and life histories, when compared to other birds. Kiwi are flightless, nocturnal, ground-dwelling birds that feed primarily on invertebrates. They belong to the paleognathous an early avian taxon comprising flightless birds (the ratites) and the tinamous (47 species in nine genera). The current paleognathous include the ostrich (Struthionidae), the rhea (Rheidae), the tinamous (Tinamidae), the cassowary (Casuariidae), the emu (Dromaiidae), and the kiwi (Apterigidae) (Mitchell et al., 2014; Yonezawa et al., 2017; Sackton et al., 2018). Previous studies showed that the ancestors of ratites were small enough to fly (Yonezawa et al., 2017) and that the loss of flight was convergent in this lineage (Sackton et al., 2018). With a size ranging from 23 kg for the smallest rhea to 111kg for the ostrich (Wilman et al., 2014), most extant ratites are remarkable for their impressive sizes. Among their extinct representatives, the moa (*Dinornis robustus*) had an estimated weight of up to 240 kg, and the elephant birds (*Aepyornis maximus*) weighed more than 500kg (Angst & Buffetaut, 2018). Surprisingly, kiwi are significantly smaller than their sister group, the elephant birds, and closer in size to the tinamous, a flying paleognath. They are only the weight of a chicken, with the female Rakiura tokoeka (*Apteryx australis*), being the largest species of kiwi, weighing up to 4 kg. Even more surprising, in spite of their small size, they have a relatively large egg, a feature also observed in the elephant bird (Yonezawa et al., 2017). Kiwi eggs can be as large as the egg of a rhea or an emu, birds that are ten times heavier (Migeon, 2014). The kiwi egg weighs up to a quarter of the female body mass and takes a huge volume in the mother's abdomen (Calder, 1979). In Brown kiwi (*Apteryx mantelli*) and Little-spotted kiwi (*Apteryx owenii*), the male broods the egg inside a nest built in a burrow during 75-84 days, one of the longest incubation periods among birds (Calder et al., 1978). From this large egg, hatches a chick that resembles an adult bird and that is nearly completely independent from just a few hours after hatching (Calder et al. 1978). In addition to the above unusual characteristics, kiwi's gait is different from that of other ratites: proportionally to their size, their steps are longer, they put their feet on the ground further forward, and to accelerate, they increase mainly the step length instead of the step frequency (Abourachid & Renous, 2000). Furthermore, compared to other ground-dwelling birds of the same size, kiwi take more time to move their foot forward to complete a step (longer swing time) (Abourachid & Renous, 2000).

In this paper, we wanted to investigate potential morphological adaptations to the strange reproductive and locomotive functions in kiwi, and understand whether and how the size of the kiwi egg influences kiwi's body shape and posture. Therefore, herein we describe the anatomy of kiwi, with a focus on the pelvis and hind limb musculoskeletal system. Then, we compare the postcranial anatomy of kiwi to that of other birds.

To understand how carrying and brooding such a huge egg affects the female and male musculoskeletal system, we used three-dimensional musculoskeletal models to compare the position of bones and muscles in different postures: standing with and without carrying an egg, as well as brooding. In light of the anatomical specificities of kiwi, we linked the musculoskeletal system shape to the functional constraints associated with carrying a huge egg. This allowed us to find causal links between the skeleton morphology, the reproductive traits and the locomotion of kiwi.

Materials and Methods

Specimens

Two frozen specimens of Little-spotted kiwi (*Apteryx owenii*), one female (n°55790) and one male (n°55789), and two specimens of male Brown kiwi (*Apteryx mantelli*) (n°54765 and n°56040) submitted for post-mortem to Wildbase, School of Veterinary Sciences, Massey University, were available for anatomical study. In this study, we only considered postcranial anatomy. The ribs were cut under the uncinate process and the viscera were removed for autopsy before freezing, but the limb muscles were intact at least on one side. After the study, the bodies were given back to Wildbase.

Bone anatomy

We identified the kiwi specific features using the character matrix provided by Livesey & Zusi (2007) who used the anatomical characteristics of bird skeletons to carry out a phylogenetic analysis. The authors defined the states of 2954 anatomical characters in 188 avian species, including several fossil species, and the genera *Apteryx* and *Struthio*. From the matrix, we extracted the number of occurrences of each state for the 2954 characters. We determined the most common states among the 188 species, and compared them to those of *Apteryx* and *Struthio*. We thus were able to identify the kiwi characters that differed from most of the other bird species, and those that differed from *Struthio*. We refer to the most common state of the each of the characters when making comparisons in the description of the anatomical characters. We paid special attention to the specific characters in our description of the lower appendicular skeleton. We followed the *Nomina anatomica avium* osteological nomenclature (Baumel & Witmer, 1993).

Muscle dissection

We performed detailed dissections on the four specimens, using the accurate description of Beddard (1899) as a reference. Following dissection, the thigh and leg muscles were photographed, removed, and weighed. We carefully referenced the origin and insertions

of the muscles during dissection. We did not dissect the tarsometatarsus and toes, but verified the function of the digit flexors during dissections. We compared the muscle anatomy, and the muscle mass proportions to those available from ostriches (Smith, 2015), emus (Lamas et al., 2014) , and turkeys (Abourachid, 1991).

Osteomuscular system 3D model reconstruction

Two specimens of Little-spotted kiwi (*Apteryx owenii*), one female (n°55790) and one male (n°55789), and one specimen of male Brown kiwi (*Apteryx mantelli*) (n°56040) were scanned using the computed tomography facility (CT), at Massey University, New Zealand (power: 90 kV, 88 mA; resolution: 0.8 mm on each axis). The CT-scan data are available for the three specimens (https://mycore.core-cloud.net/index.php/f/902106517). We used Avizo (version 6.3; FEI Visualization Sciences Group) to reconstruct bone models from the CT scans and imported the models in obj file format into Autodesk Maya (2018, Autodesk Inc., San Rafael, CA, USA).

We observed mounted kiwi skeletons at Massey University at Palmerston North and at the Muséum National d'Histoire Naturelle (MNHN) osteological collection (specimen MNHN 2012-194) to complement information on missing ribs. Radiographies of a gravid alive Brown kiwi (Calder, 1979) and of a non-gravid alive Brown kiwi (Massey University), as well as our observations of a brooding kiwi bird were used to approximate the position of the Brown kiwi bones in these three postures using Autodesk Maya software.

Although there were no significant differences between the Little-spotted and the Brown kiwi anatomy, the proportions were different between the bones of these two species, making the 3D model construction more difficult using a female Little-spotted kiwi bones to match Brown kiwi radiographies. Therefore, we scaled the bones of a male Brown-kiwi to build our models in Autodesk Maya software.

Following our observations during dissections, we determined a point that corresponded to the geometrical centre of the origin, and of the insertion areas of each muscle on the bones. We represented each dissected muscle by a cylinder attached to the bone by these geometric centres. For a given muscle, the cylinder diameter corresponded to the percentage mass of the muscle in relation to the total limb muscle mass. As muscles were attached virtually (i.e. using the software) to the bones, they passively increased or decreased in length to fit the new 3D position in Autodesk Maya.

Results

There were no differences in the overall anatomy of the two dissected species (Little-spotted and Brown kiwi) or between sexes. Moreover, as the radiographies were available for Brown kiwi, we decided to focus our description on this species. We provide the quantification of the relative muscle sizes (Supplementary Material SM1) for each specimen and 3D bone models (Supplementary Material SM2) for a specimen of Brown kiwi.

Osteology

- Thorax and pectoral girdle

On the thoracic area, the ribs were wide with large uncinate processes. The ventral ribs were small and attached on a small and flat sternum. The pectoral girdle was typical of flightless birds, with vestigial wing bones. The coracoid was very short and the scapula anchored on the muscles laterally on the ribs, at the level of the uncinate process of the first thoracic rib. The thoracic rib was closed rather anteriorly (Supplementary Material SM2).

- Synsacrum and pelvis

Cranially, the synsacrum aligned with the thoracic vertebrae, which are virtually horizontal when standing. The synsacrum was curved ventrally (Fig. 1A). The curvature was slight in the preacetabular part and more marked in the fused caudal vertebrae. Caudally, the free caudal vertebrae were nearly vertical in a standing position (Fig. 1A).

The vertebrae spinal processes were as high on the synsacrum as on the thoracic vertebrae. The transverse processes were very short, even near the acetabulum and absent in the most caudal part, as on the free caudal vertebrae. There was no transverse lamina on the pelvis (Fig. 1).

The two iliac alae were projected cranially (Fig.1) on the last thoracic vertebrae so that two ribs were lying under the pelvis (Supplementary Material SM2). On the cranial part of the pelvis the iliac ala were separated dorsally and curved laterally to cover the ribs. The two iliac alae joint dorsally above the synsacrum and the pelvis was compressed laterally. Caudally to the antitrochanter, the ilium was short and narrow, laterally compressed, so that it covered only the spinal process of the fused caudal vertebrae. The vertebral body extended ventrally to the ilium.

The ilium and ischium were only fused anteriorly, around the acetabulum (Fig. 1, Supplementary Material SM2). The ilioischiatic fenestra was very large. A membrane between the ilium and the ischium covered the lateral side of the vertebrae and closed the ilioischiatic fenestra. Cranially, this membrane did not join the corpus ischii, leaving space for nerves and vessels.

The ischium body formed the caudoventral wall of the acetabulum when standing. Its dorsal extremity joined the ventral part of the antitrochanter. A lateral process extended laterally under the antitrochanteric part of the ilium. The ischium corpus was oblique medially. The scapus formed a blade extending caudally, medially to the antitrochanter. It was oriented downward, almost vertically when standing.

The corpus pubis was small. It joined the ilium ventrally toward the acetabulum and joined the ilium corpus cranially. The scapus pubis was oriented dorsoventrally, almost vertical when standing. A membrane closed the puboischiatic fenestra. Both the pubis and the ischium were longer than the post acetabular part of the ilium.

- Femur

The femoral diaphysis was incurved craniodistally on a lateral perspective (Fig. 2A). The distal extremity of the femur was asymmetrical, the medial condyle extended distally and ventrally (Fig. 2B). The condyle were sub-equal on the dorsal side.

- Tibiotarsus

The proximal extremity of the tibiotarsus was virtually planar with no elongation of the cnemial crest, the fibula extended cranially (Fig. 2C). At the distal extremity of the tibiotarsus, the medial condyle was distinctly more cranially prominent than the lateral condyle. The lateral and medial margins were not parallel. (Fig. 2D).

- Tarsometatarsus

At the proximal extremity of the tarsometatarsus, the intercondylar eminence was well developed and the hypotarsal sulcus was open (Fig. 2E). The plantar face of the tarsometatarsus diaphysis was flat.

Myology

The muscle name synonymy between Berge (1982) and McGowan (1979) is given for the proximal (table 1) and distal hind limb muscles (table 2) with the description of origins and insertions. The location of the muscles on the hind limb is shown in Figure 3. The location of the origins and insertions of the muscles is shown on the pelvis (Fig. 4), femur (Fig. 5), tibiotarsus (Fig. 6), and proximal part of the tarsometatarsus (Fig. 7).

The thigh muscle *caudofemoralis* has a remarkable shape. The insertion of its *pars pelvica* is located along the entire femur caudal face (Fig. 3B, Fig. 5D), whereas when present in other birds, it inserts proximally on the femur (Baumel, 1993; Smith et al., 2006; Lamas et al., 2014).

Its *pars caudalis* originates all along the free caudal vertebrae, i.e., all along the tail (Fig.3C, Fig. 5D), whereas it usually inserts on the uropygium (Baumel & Witmer, 1993).
The proportion and orientation of the other muscles vary in comparison with other species, but the bone attachments are similar. The relative mass of this muscle is similar in the kiwi and the turkey, while it is relatively smaller in the ostrich (SM1).

3D model reconstruction
The static 3D model of a brown kiwi osteomuscular system in a standing position with and without an egg and in the brooding position are given Figure 8 and Figure 9, respectively.

Discussion

Anatomical specificities of the kiwi osteology.

- Pectoral girdle

The kiwi skeleton presents several unusual features. Their vestigial wings are the most reduced among extant birds. Moreover, the width of the vertebral ribs are larger than the intercostal spaces, which is a trait only shared with the hoatzin (*Opisthocomus hoatzin*) (Livesey & Zusi, 2007). The hoatzin stays most of its time perched on branches, laying on its sternal keel (Strahl, 1988). Considering the anatomical similarity with this bird, we can assume that the ribs of kiwi are enlarged to support body weight as well. Interestingly, during the brooding period, the male Brown kiwi develops well-defined brood patches (Colbourne, 2002), an area of featherless skin on the ventral side of an incubating bird. The avian brood patch is supplied with superficial blood vessels, making it possible for the incubating parent to transfer heat to the egg. In Brown kiwi, the brood patch usually lies to the back of a ventral line between the vestigial wings and covers the ventral body to about 50mm from the cloaca. It is usually about 10cm wide x 12cm long (Colbourne, *pers. comm.*). The Brown kiwi egg length is on average 12.8 ± 0.5cm (n = 15) (IC *unpub. data*). Thus, to be able to cover such large egg with the brood patch, the incubating parent (male or female) needs to lean its body on the egg, as shown by our 3D musculoskeletal model (Fig. 9). Therefore, we can assume that the kiwi ribs are enlarged to support the body weight when leaning on the egg, as it is for the hoatzin leaning on its branch.

- Pelvis

The ratite pelvis is laterally compressed in both its preacetabular and post acetabular parts (Baumel & Witmer, 1993) (Fig. 1, SM3). In most neognaths, except diving neognaths (Anten-Houston et al., 2017), the ilia is usually separated by the synsacrum, which is enlarged at the post acetabular region leading to the two ilia being widely separated (SM3) (Baumel & Witmer, 1993). Moreover, in ratites, the ilioischiatic fenestra is open and the ischium is narrower than

244 in most neognaths. In ratites, ilium and ischium are not fused, and the ischium is longer than
245 the ilium. Considering these features, the overall shape of the kiwi pelvis is typical of ratites.
246 However, the kiwi synsacrum is bent downward, whereas it is straight in both the ostrich and
247 the turkey. In kiwi, the free caudal vertebrae are oriented downward and the tailbones forms a
248 rigid stick, whereas the tail of other birds is usually mobile. This specific caudal part of the kiwi
249 pelvis could help to maintain the egg in gravid females, and both sexes may rest on the rigid
250 stick-like tail when roosting.
251 Moreover, kiwi have a pronounced lateral compression of the post acetabular part of the pelvis.
252 The two iliac crests were in contact medially, in contrast to the ostrich, where the post
253 acetabular iliac alae are separated by the synsacrum and the dorsal part of the ilia are dorsally
254 enlarged (Fig 1, SM3). This narrow pelvis does not allow carrying the large egg between the ilia
255 and pubis, close to the rachis, as it is the case in other birds (Shatkovska et al., 2018). Therefore,
256 in kiwi, the egg is carried ventrally below the pelvis. The last thoracic vertebrae allows a slight
257 dorsal flexion of the pelvis, clearly seen on the radiography (Calder, 1979) (Fig. 8A). All the
258 viscera had to be contained in the cranial part of the ribcage, thus the sternal ribs and the
259 sternum seem to be push forward.
260 The narrow pelvis is a feature usually associated with an abducted femur, as observed in diving
261 (Hertel et al., 2007; Anten-Houston et al., 2017) and paddling birds (Provini et al., 2012, 2013).
262 However, in contrast to most diving birds (except guillemots and penguins (Shufeldt, 1901)
263 and crex, rallus, and phasianus (Bogdanovich, 2014)), kiwi post acetabular ilium is short, with
264 a downward orientation of the synsacrum and a downward orientation of the ischium
265 (Shatkovska et al., 2018). The cranial projection of the iliac ala, the short post acetabular ilium,
266 the bending of the vertebral column, and the large ilioischiatic fenestrae contribute to the
267 ventral bending of the pelvis and the posterior position of the hip on the body. The hip needs
268 to be flexed and the femur abducted to bring the knees on each side of the body, even when
269 carrying a large egg.
270
271 - Limb
272 The overall shape of the limb bones looks like those of ground-dwelling birds (Fig. 2F).
273 Although bones' proportions are similar to neognath birds, and therefore different from the
274 other ratites (Gatesy & Middleton, 1997). For example, the tarsometatarsus is short (25% leg
275 length) in contrast to those of other ratites (40% of the leg length) (Gatesy & Middleton, 1997).
276 The short bones, associated with a flexed posture (Fig. 8) (Abourachid & Renous, 2000), keep
277 the centre of mass close to the ground. In addition, the toes are strong, with no reduction unlike
278 in the other ratites. These features contribute to increase the stability of kiwi, while walking in
279 a complex habitat, and is shared by other burrowing animals (Kardong, 1995).

The long axis curvature of the kiwi femur is unique (Cracraft, 1974) and the length of the fibular crest is only shared with the emu (*Dromaius*) and the cassowary (*Casuarius*) (Livesey & Zusi, 2007). In kiwi, the long fibular crest together with the long axis curvature of the femur turns the rotation axis of the knee horizontally, in a standing posture when the femur is abducted (Fig 2F, SM 2). The tibial plateau is flat in kiwi and the fibular head protrudes laterally onto the lateral face of the femoral condyle. This contributes to the cohesion of the knee joint, preventing the lateral dislocation of the tibiotarsus even when it is adducted, to bring the ankle joint closer to the sagittal plane (Fig 2F). On the distal epiphysis of the tibiotarsus, the medial condyle is larger than the lateral one. Due to this asymmetry of the condyles, the rotation axis of the ankle joint is horizontal and the tarsometatarsus is vertical on standing position.

The above adjustments of the shape of each limb segment permit a standing posture with a flexed hip, an abducted femur, an adducted tibiotarsus, and a sub-vertical tarsometatarsus. Thus, despite a very narrow pelvis, the knees can move without the distal part moving too laterally, keeping the feet close to the sagittal plane, under the body. Moreover, the limb features contribute to the kiwi rounded body morphology. Due to the backward curvature of the post acetabular pelvis, the hips are located at the caudal end of the body. The relatively long femur (31% leg length) on the much-flexed hip bring the knee cranially and dorsally (Fig. 2F). The tibiotarsus proportion (44% leg length) is larger than in other ratites (35-45%) (Gatesy & Middleton, 1997). It allows to keep the ankle joint down on the side of the trunk and to assure enough displacement during walking. As it is the case for other burrowing vertebrates (eg Emerson, 1976; Warburton, 2003; Ilyinsky, 2008) the tarsometatarsus is short (25% leg length) and the toes well developed and strong. This suggests kiwi could use their feet for excavating soil, for example when digging their nests.

The proportions of the leg segments and the high hip flexion have consequences on the walking gait. At the same speed relatively to their size (hip height), the kiwi walks at lower frequencies (i.e. relatively slower motion,), and longer strides relative to the other ratites (Abourachid & Renous, 2000). The flexed hip limits the craniocaudal motion of the knee because the hip extension moves the knee downward rather backward. This explains why the long tibiotarsus permits to bring the foot forward, but as the knee is cranial, the foot cannot be brought caudally, which is also a specific trait of the kiwi gait (Abourachid & Renous, 2000).

Anatomical specificities of the kiwi myology.

One striking muscle feature observed during dissection was the unique shape of a thigh muscle, the *caudofemoralis*. The insertion of its *pars pelvica* is located along the entire femur caudal face (Fig. 3B, Fig. 5D), whereas when present in other birds, it inserts proximally on the femur (Baumel, 1993; Smith et al., 2006; Lamas et al., 2014). The *pars pelvica* thus participates to the femur extension. Moreover, when co-contracted with antagonist extensors, it could form a

second muscular layer parallel to the abdominal wall. Therefore, the *caudofemoralis pars pelvica* could help the infrapubic muscles to maintain the abdominal wall during gestation. This role is also played by the pelvic ilioischiatic and ischiopubic membranes, which increase the limb muscles' insertion areas and hold the infrapubic muscles (Fechner et al., 2013).

Its *pars caudalis* originates all along the free caudal vertebrae, i.e., all along the tail (Fig.3C, Fig. 5D), whereas it inserts on the uropygium in the other birds (Baumel & Witmer, 1993). Interestingly, the kiwi uropygium wraps around the caudal vertebrae in contrast to other birds where it is restricted to the pygostyle region (Reynolds et al., 2017). The *pars caudalis* pulls on the tail and brings it cranially under the trunk, potentially playing a role holding the egg in gravid females (Fig. 8). This specific insertion of the *caudofemoralis pars caudalis* could take part in the downward orientation of the caudal vertebrae. This downward orientation of the post acetabular pelvis and tail is likely to help the infrapubic muscles to surround the egg in the abdominal cavity. However, as previously seen, this pulls the hip backwards and causes the hip to flex and the femur to be abducted to sufficiently carry the knee forward. The proportion and orientation of the other muscles vary in comparison with other species, but the bone attachments are similar. The previously discussed distinctive features of the kiwi pelvis' shape contribute to the differences in the topology of the muscles' attachments. For instance, the *Ischiofemoralis* originated from the ischium both in turkey and kiwi (SM3), but the different bone position and proportions led to a different relative position of the origin between species. The relative mass of this muscle is similar in the kiwi and the turkey, while it is relatively smaller in the ostrich (SM1). Surprisingly, despite the differences in the topology of the muscle attachments due to the specific shape of the ratite pelvis, the proportion of the leg muscle mass differs less between the kiwi and the turkey (Abourachid, 1991) than between the kiwi and the ostrich (Smith et al., 2006). Although the sum of the differences between the relative muscle masses of the kiwi and of the ostrich is 52%, it is only 29% between the kiwi and the turkey (SM1). The ostrich is not considered a ground-dwelling bird but a cursorial bird (Abourachid & Renous, 2000). Specific adaptations can be observed, as the lengthening and the mass reduction of the distal part of the leg (Abourachid & Renous, 2000). In addition, the number of toes is reduced, as in horses, considered as typical cursorial mammals (Alexander, 1982). Thus, despite a closer phylogenetic relationship between the ostrich and the kiwi, the functional demand for cursorial versus ground-dwelling locomotion is a strong constraint, which can affect muscle proportions and explain the differences observed between the ostrich and the kiwi on one hand and the turkey and kiwi on the other hand. In addition, the lack of differences between males and females anatomy in the two analyzed kiwi species also suggests that the selective pressure on locomotion is stronger than the selective pressure on egg transport, which provides important insights into evolutionary processes.

Conclusion

The kiwi is a small and burrowing bird. Its egg is disproportionally large and this reproductive feature imposes mechanical constraints on the musculoskeletal system. As the pelvis is not wide enough to hold the egg, it is carried in front of the pelvis. The post acetabular part of the body (pelvic and tail) is curved downward, which could help to maintain the egg. The hips are flexed and the femur abducted, holding the knees high on the side of the body. The tibiotarsus is rather long, participating to the motion of the legs. The tarsometatarsus is short, and the feet are strong as usually is in burrowing animals. The body shape, as well as the peculiar gait parameters of the kiwi are a tradeoff between two functions: the reproduction and the locomotion.

365

366 **References**

367 **Abourachid A** (1990) *Etude morpho-fonctionnelle de l'appareil locomoteur de deux souches*
368 *de dindons domestiques: Recherche d'une explication fonctionnelle aux boiteries des*
369 *dindons ultra-lourds*, Université Rennes 1.

370 **Abourachid A** (1991) Myologie du membre pelvien du dindon domestique Meleagris
371 gallopavo. *Anat Histol Embryol* **20**, 75–94. doi:10.1111/j.1439-0264.1991.tb00294.x.

372 **Abourachid A, Renous S** (2000) Bipedal locomotion in ratites (Paleognatiform): examples
373 of cursorial birds. *Ibis (Lond 1859)* **142**, 538–549. doi:10.1111/j.1474-
374 919X.2000.tb04455.x.

375 **Alexander RM** (1982) Walking, Running and Jumping. In *Locomotion of Animals*.
376 Dordrecht: Springer Netherlands, 81–113. doi:10.1007/978-94-011-6009-4_5.

377 **Angst D, Buffetaut É** (2018) *Paléobiologie des oiseaux géants terrestres*, ISTE Editions.

378 **Anten-Houston M V, Ruta M, Charles D** (2017) Effects of phylogeny and locomotor style
379 on the allometry of body mass and pelvic dimensions in birds. doi:10.1111/joa.12647.

380 **Baumel JJ** (1993) Handbook of avian anatomy: nomina anatomica avium. *Publ Nuttall*
381 *Ornithol Club (USA) no 23*.

382 **Baumel JJ, Witmer L** (1993) *Handbook of avian anatomy*, Nuttall Ornithological Club.

383 **Beddard FE** (1899) Notes on the anatomy of the genus Apteryx. *Novit Zool* **6**, 386–402.

384 **Berge JC Vanden** (1982) Notes on the myology of the pelvic limb in kiwi (Apteryx) and in
385 other birds. **99**, 309–315.

386 **Bogdanovich IA** (2014) Morphoecological peculiarities of pelvis in several genera of rails
387 with some notes on systematic position of the coot, fulica atra rallidae, gruiformes. *Vestn*
388 *Zool* **48**, 249–254. doi:10.2478/vzoo-2014-0028.

389 **Calder WA** (1979) The Kiwi and Egg Design: Evolution as a Package Deal. *Bioscience* **29**,
390 461–467.

391 **Calder WA, Parr CR, Karl DP** (1978) Energy content of eggs of the brown kiwi Apteryx
392 australis; an extreme in avian evolution. *Comp Biochem Physiol -- Part A Physiol* **60**,
393 177–179. doi:10.1016/0300-9629(78)90226-8.

394 **Colbourne R** (2002) Incubation behaviour and egg physiology of kiwi (Apteryx spp.) in
395 natural habitats. *N Z J Ecol* **26**, 129–138.

396 **Cracraft J** (1974) Phylogeny and evolution of the ratite birds. *Ibis (Lond 1859)* **116**, 494–521.
397 doi:10.1111/j.1474-919X.1974.tb07648.x.

398 **Emerson SB** (1976) Burrowing in frogs. *J Morphol* **149**, 437–458.
399 doi:10.1002/jmor.1051490402.

400 **Fechner R, Stratmann M, Gößling R, et al.** (2013) The functional role of the ischiopubic
401 membrane for the mechanical loading of the pubis in the domestic fowl (Gallus gallus). *J*

402 *Anat* **222**, 305–312. doi:10.1111/joa.12015.
403 **Gatesy SM, Middleton KM** (1997) Bipedalism, flight, and the evolution of theropod
404 locomotor diversity. *J Vertebr Paleontol* **17**, 308–329.
405 **Hertel F, Campbell Jr KE, James HF** (2007) The antitrochanter of birds: form and
406 function in balance. *Auk* **124**, 789–805.
407 **Ilyinsky VA** (2008) Locomotor Adaptations in the Hindlimbs of Owls: the Burrowing Owl
408 (Athene cunicularia), compared to the Little Owl (Athene noctua). *Oryctos* **7**, 267–272.
409 **Kardong K V** (1995) *Vertebrates: comparative anatomy, function, evolution*,
410 **Lamas LP, Main RP, Hutchinson JR** (2014) Ontogenetic scaling patterns and functional
411 anatomy of the pelvic limb musculature in emus (Dromaius novaehollandiae). *PeerJ* **2**,
412 e716. doi:10.7717/peerj.716.
413 **Livesey BC, Zusi RL** (2007) Higher-order phylogeny of modern birds (Theropoda, Aves:
414 Neornithes) based on comparative anatomy. *Zool J Linn Soc* **149**, 1–95.
415 **McGowan C** (1979) The hind limb musculature of the brown kiwi, Apteryx australis mantelli.
416 *J Morphol* **160**, 33–73. doi:10.1002/jmor.1051600105.
417 **Migeon A-S** (2014) *Anatomie comparée des ratites*, Université Paul Sabatier, Toulouse,
418 Toulouse. doi:10.1016/j.geoderma.2008.11.037.
419 **Mitchell KJ, Llamas B, Soubrier J, et al.** (2014) Ancient DNA reveals elephant birds and
420 kiwi are sister taxa and clarifies ratite bird evolution. *Science (80-)* **344**, 898–900.
421 doi:10.1126/science.1251981.
422 **Provini P, Goupil P, Hugel V, et al.** (2012) Walking, paddling, waddling: 3D kinematics
423 Anatidae locomotion (Callonetta leucophrys). *J Exp Zool Part A Ecol Genet Physiol* **317**,
424 275–282.
425 **Provini P, Simonis C, Abourachid A** (2013) Functional implications of the intertarsal
426 joint shape in a terrestrial (Coturnix coturnix) versus a semi-aquatic bird (Callonetta
427 leucophrys). *J Zool* **290**, 12–18. doi:10.1111/jzo.12007.
428 **Reynolds SM, Castro I, Alley MR, et al.** (2017) Apteryx spp. (Kiwi) possess an uropygial
429 gland: Anatomy and pathology. *Eur J Anat* **21**, 125–139.
430 **Sackton TB, Grayson P, Cloutier A, et al.** (2018) Convergent regulatory evolution and
431 the origin of flightlessness in palaeognathous birds. *bioRxiv*, 262584.
432 doi:10.1101/262584.
433 **Shatkovska O V, Ghazali M, Mytiai IS, et al.** (2018) Size and shape correlation of birds'
434 pelvis and egg: Impact of developmental mode, habitat, and phylogeny. *J Morphol* **279**,
435 1590–1602. doi:10.1002/jmor.20888.
436 **Shufeldt RW** (1901) *Osteology of the Penguins*,
437 **Smith DK** (2015) Craniocervical myology and functional morphology of the small-headed
438 therizinosaurian theropods Falcarius utahensis and Nothronychus mckinleyi. *PLoS One*

10, 1–16. doi:10.1371/journal.pone.0117281.

Smith NC, Wilson AM, Jespers KJ, et al. (2006) Muscle architecture and functional anatomy of the pelvic limb of the ostrich (Struthio camelus). *J Anat* **209**, 765–779. doi:10.1111/j.1469-7580.2006.00658.x.

Strahl SD (1988) The social organization and behaviour of the Hoatzin Opisthocomus hoazin in central Venezuela. *Ibis (Lond 1859)* **130**, 483–502. doi:10.1111/j.1474-919X.1988.tb02714.x.

Warburton N (2003) Functional morphology and evolution of marsupial moles (Marsupialia: Notoryctemorphia).

Wilman H, Belmaker J, Simpson J, et al. (2014) EltonTraits 1.0: Species-level foraging attributes of the world's birds and mammals: Ecological Archives E095-178. *Ecology* **95**, 2027.

Yonezawa T, Segawa T, Mori H, et al. (2017) Phylogenomics and Morphology of Extinct Paleognaths Reveal the Origin and Evolution of the Ratites. *Curr Biol* **27**, 68–77.

Acknowledgment

We are thankful to the Action Transversale du Muséum (ATM) for providing financial support. Thanks to Nicola Moffatt and Brett Gartrell for their help with the CT-scans.

Authors Contributions

AA, IC and PP participated in the design of the paper. IC provided the material and facility to acquire the data, AA and PP proceeded to the data acquisition (dissections), and PP built the musculoskeletal models. AA and PP contributed to the data interpretation. AA, IC, and PP drafted and made critical revisions of the manuscript. All authors approved the article.

Competing interests

The authors declare no conflict of interests.

Data accessibility

The CT-scan data of two specimens of Little-spotted kiwi (*Apteryx owenii*), one female (n°55790) and one male (n°55789), as well as one specimen of male Brown kiwi (*Apteryx mantelli*) (n°56040) are available at https://mycore.core-cloud.net/index.php/f/902106517. The Maya scene with the 3D musculoskeletal models is available at https://mycore.core-cloud.net/index.php/f/902116552.

Tables

475 Table 1 Proximal hind limb muscles dissected, alternate names in other sources, and
476 description of their origins and insertions. The left most column shows the muscles used in
477 this study with their names abbreviated. The second and third columns identify alternate
478 names used in major avian myology works (Baumel & Witmer, 1993). The fourth and fifth
479 columns provide a description of the origin and insertion of the muscles, respectively.
480

Abbreviation	Vanden Berge & Zweers	McGowan	Origin	Insertion
Iliotib cran	*iliotibialis cranialis*	*M. sartorius*	cranio dorsal edge ilium	medial part patellar tendon
Iliotib lat	*iliotibialis lateralis*	*M. iliotibialis*	dorsal edge ilum	cranial and lateral part patellar tendon
Iliotroch cran	*iliotrochantericus cranialis*	*M. iliotrochan tericus an terior*	ventral edge preacetabular ilium	lateral proximal femoral epiphysis
Iliotroch med	*iliotrochantericus medius*	*M. iliotrochantericus medius*	ilium cranio ventral to acetabulum	
Iliotroc cau	*iliotrochantericus caudalis*	*M. iliotrochantericus posterior*	all depression preacetabular ilium surface	proximal lateral femoral epiphysis
Iliofib	*iliofibularis*	*M. biceps femoris*	dorsal edge of the ilium from the antitrochanter area to most of the preacetabular part	through a ligamentar loop on a lateral tuberculeon the proximal 1/3 fibula
Iliofem ext	*iliofemoralis externus*	*M. gluteus medius et minimus*	dorsal ilium antitrochanter	lateral femur proximal epiphysis
Flex cru lat pelv	*flexor cruris lateralis pars pelvica*	*M. semitendinosus*	caudal part of the ilium	proximal tibio by flat thin tendon betwen Gastrocnemius lateralis and intermedia
Flex cru lat acc	*flexor cruris lateralis pars accesoria*		distal caudal part of the femur	
Caudofem cau	*caudofemoralis caudalis*	*M. piriformis pars caudofemoralis*	all the caudal vertebrae	femur posterior proximal shaft
Caudofem pelv	*caudofemoralis pelvica*	*M. piriformis pars iliofemoralis*	synsacrum ventral to the ilium	caudal part of the femur, just distally to the caudoofemoralis caudalis insertion, medial to and all along the femorotibialis lateralis origin
Ischiofem	*ischiofemoralis*	*ischiofemoralis*	ilioischiatic membran and ischium	lateral proximal femoral epiphysis
Obt int	*obturatorius internus*	*M. obturator internus*	visceral side of the pelvis, on the ilioischiatic membran	lateral proximal femoral epiphysis
Amb	*ambiens*	*M. ambiens*	preacetabular part of the pubis	Patella (F) tendon through the patella to the tibiotarsus (M)
Pub isch fem	*pubo- ischio-femoralis*	*M. adductor longus et brevis*	all length of the ischium (F) and pubis (M)	femur along lateral face to the medial trochlea

481
482

Table 2 Distal hind limb muscles dissected, alternate names in other sources, and description of their origins and insertions. The left column shows abbreviations used in this study. The second and third columns identify alternate names used in major avian myology works (Baumel & Witmer, 1993). The fourth and fifth columns provide a description of the origin and insertion of the muscles, respectively.

Abbreviation	Vanden Berge & Zweers	McGowan	origin	insertion
Femtib lat	*femorotibialis lateralis*	*M. femorotibialis externa*	lateral and cranial surface of femoral diaphysis	mediocranial, cranail and lateral face of the patella
Femtib int	*femorotibialis internus*	*M. femorotibialis internus*	femur, mediocaudal surface	on the tibial crest by a tendon below the patelar ligament, and by fibers on gastrocnemius medialis
Femtibmed	*femorotibialis medius*	*M. femorotibialis medius*		
Fib long	*fibularis longus*	*M. peroneus longus*	medial part of the patelar ligament, and by a thin profond aponevrosis on the proximal part of the tibialis cranialis and extensor digitorum longus.	long tendon lateral that cross the tarsometatarsal joint and inserts on the proximo lateral part of the itbiotarsus. A n accessorial part of the tendon inserts on the tibila cartilage lateraly
Ext dig long	*Extensor digitorum longus*	*M. extensor digitorum longus*	from the sulcus intercnemial to the 1/3proximal of hte frontal surface of hte tibiotarsus	by a tendon restrained by a fibrous reticunaculum with the tibialis cranialis then pass in the osseous canal distal on the tibiotarsus and cross the tarsometatarsal joint and insert dorsally on digiti II,III and IV
Tib cran	*tibialis cranialis*	*M. tibialis anterior*	by a tendon on the lateral condyle of the femur and by fleshy fibres on the cnemial crest and a thin caput on the proxiaml third of the tibiotarsus	by a tendon restrained by a fibrous reticunaculum with the extensor digitorum longus and inserts on the tarsometatarsus
Gast med	*gastrocnemius medialis*	*M. gastrocnemius pars interna*	craniomedial proximal part of the tibiotarsus, below the cnemial crest	long tendon merged with the intermedia tendon to form the achille tendon
Gast int	*gastrocnemius intermedia*	*M. gastrocnemius pars media*	deeply associated with the flexor cruris medialis pars accessoria by an aponevrosis from the lateral surface of the tibiotarsus,	long tendon merged with gastrocnemius medialis tendon then to the gastrocnemius lateralis tendon to form the achille tendon

Gast lat	*gastrocnemius lateralis*	*M. gastrocnemius pars externa*	by a tendon, from laterodistal part of the femu diaphysis	
Flex ppd II	*Flexor perforans et perforatus digiti II*	*M. flexor perforans et perforatus digiti II*	by a tendon on the laterodistal part of the femur, and to the tibial part of the iliofibularis loop	
Flex ppdiii	*Flexor perforans et perforatus digiti III*	*M. flexor perforans et perforatus digiti III*	on the fibula and in the male, to the tibial part of the iliofibular loop	
Flex pdii	*Flexor perforatus Digiti II*	*M. flexor perforatus digiti II*	the fibres are threated together and share deep aponevrosys. Origin proximal on the plopiteal depession on the distocaudal part of the femur	plantar on the digit II
Flex pdiii	*Flexor perforatus Digiti III*	*M. flexor perforatus digiti III*		plantar on the digit III
Flex pdiv	*Flexor perforatus Digiti IV*	*M. flexor perforatus digiti IV*		plantar on the digit IV
Fib brev	*fibularis brevis*	*M. peroneus brevis*		plantar surface of the digits
Flex dig long	*Flexor digitorum longus*	*M. flexor digitorum longus*	caudolateral part of the tibiotarsus and on the fibula.	on the platar face of the digits
Plant	*plantaris*	*M. plantaris*	caudomedial proximal part of the tibiotarsus	by a tendon on the medial part of the tibial cartilage

Figure legends

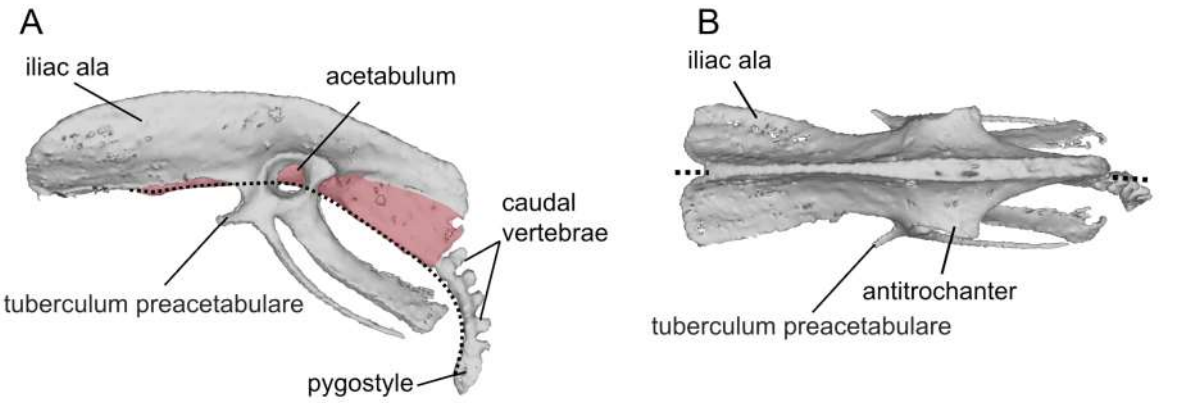

Figure 1

Osteology of the pelvis and caudal vertebrae of a Brown kiwi (*Apteryx mantelli*) lateral view with synsacrum colored in red (A), dorsal view (B). The dotted line highlights the vertebral column. The synsacrum is highlighted in red on the lateral view.

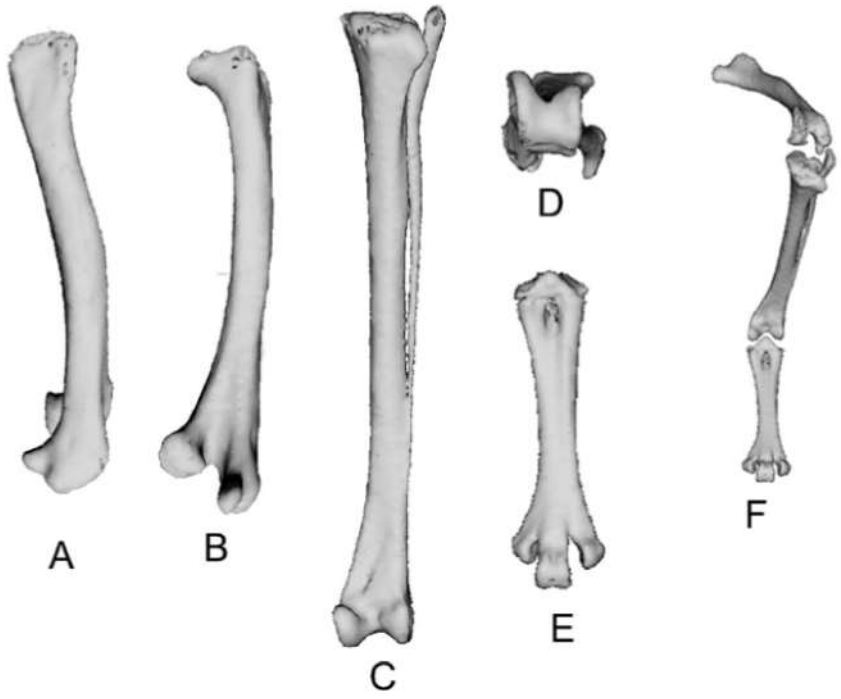

Figure 2

Osteology of a brown kiwi (*Apteryx mantelli*). Femur lateral view (A) and caudal view (B), Tibiotarsus frontal view (C), tibiotarsus distal view (D), tarsometatarsus cranial view (E), and the entire limb bones in a standing position with a frontal view (F).

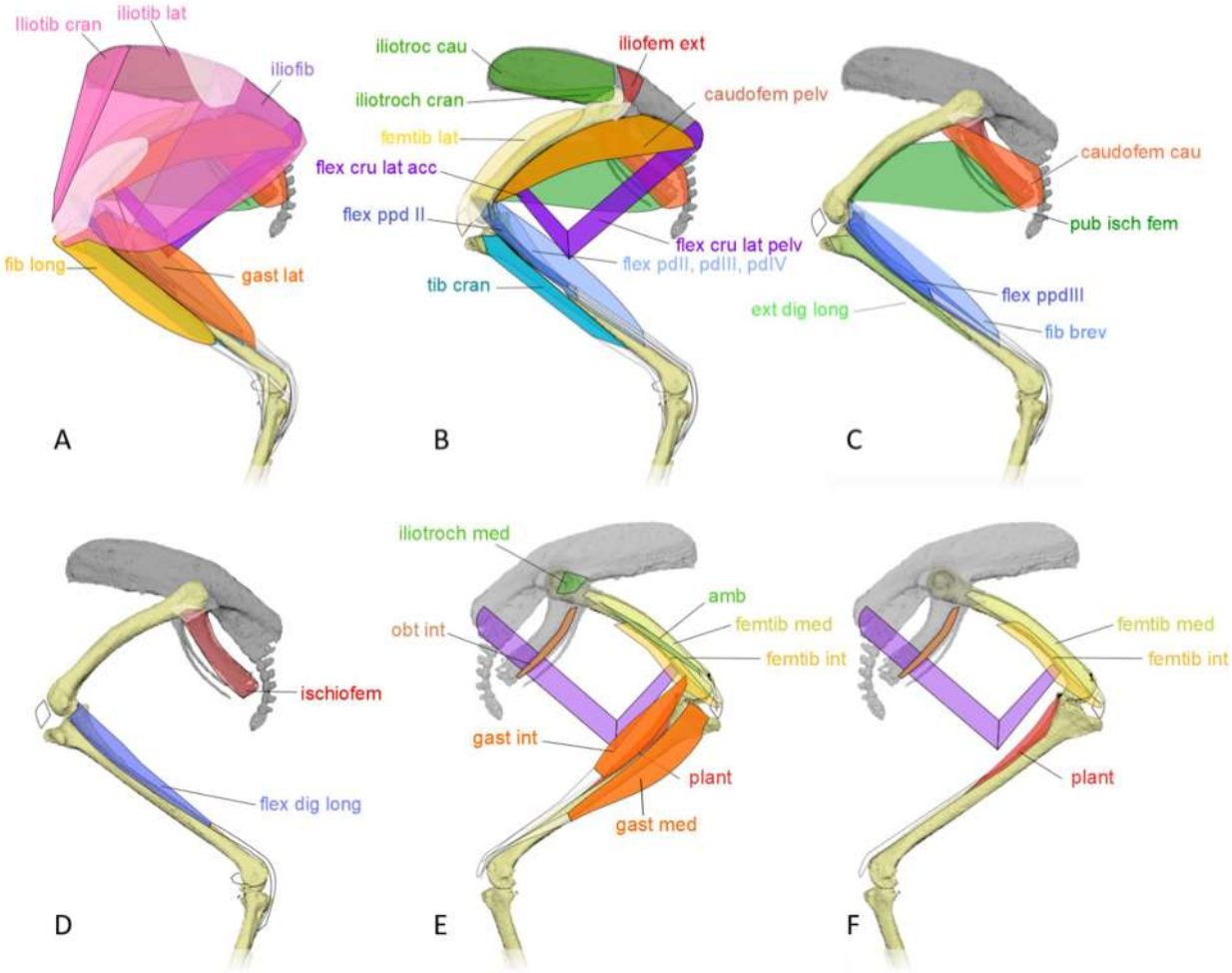

Figure 3

Location of the hind limb muscles on a specimen of a brown kiwi (*Apteryx mantelli*). The different muscle layers are represented on the lateral view (A, B, C, and D) and on the medial view (E and F), from the more superficial muscle layer on the left, to the deepest layer on the right. Abbreviations follow table 1 and table 2.

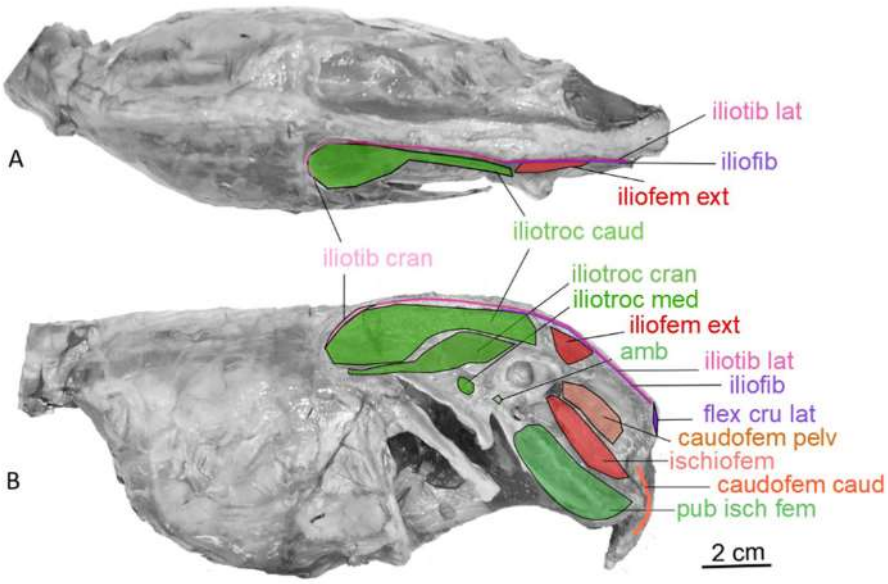

Figure 4

Muscle origins and insertions on the pelvis of a Brown kiwi (*Apteryx mantelli*) dorsal view (A) and lateral view (B). Abbreviations follow table 1 and table 2.

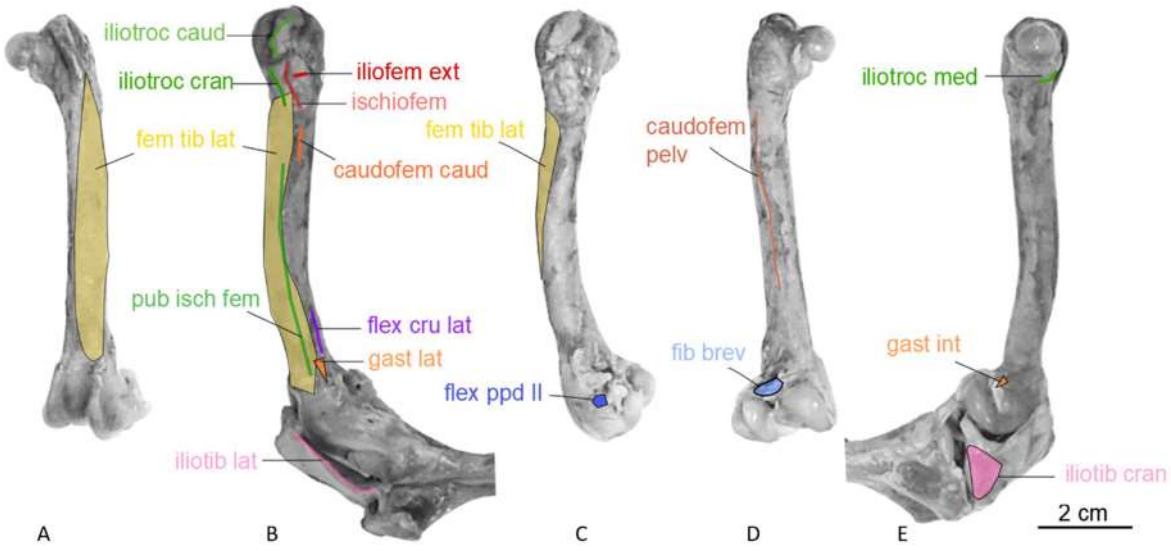

Figure 5

Muscle origins and insertions on the femur of a Brown kiwi (*Apteryx mantelli*) on the cranial (A), lateral (B), latero-caudal (C), caudal (D), and medial views (E). Abbreviations follow table 1 and table 2.

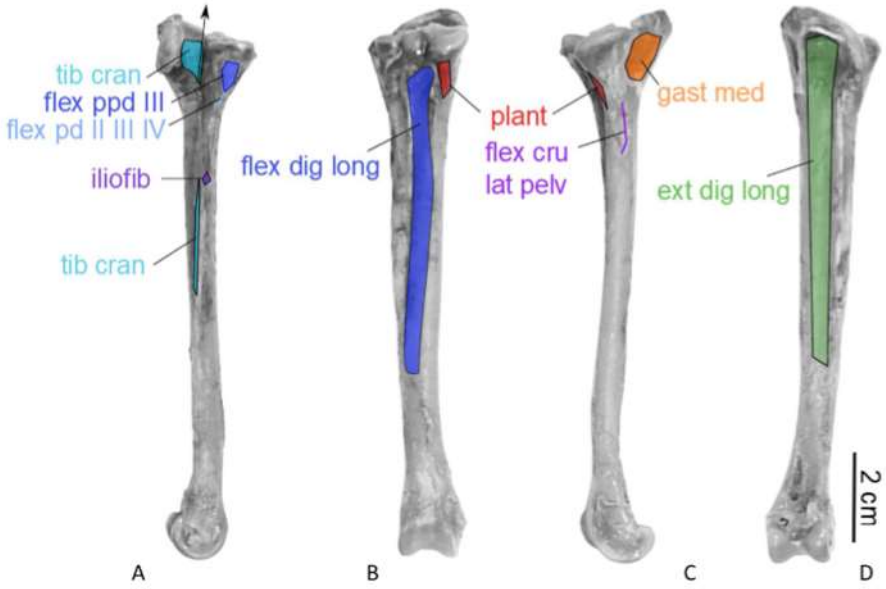

Figure 6

Muscle origins and insertions on the tibiotarsus of a brown kiwi (*Apteryx mantelli*), on the lateral (A), caudal (B), medial (C), and cranial views (D). Abbreviations follow table 1 and table 2.

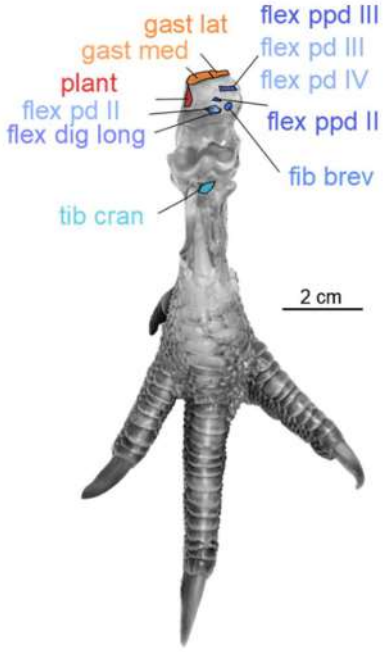

Figure 7

Position of the muscles' tendons through the tarsometatarsal joint, and insertion of the *tibialis cranialis* muscle on the cranial face of the tarsometatarsus. Abbreviations follow table 1 and table 2.

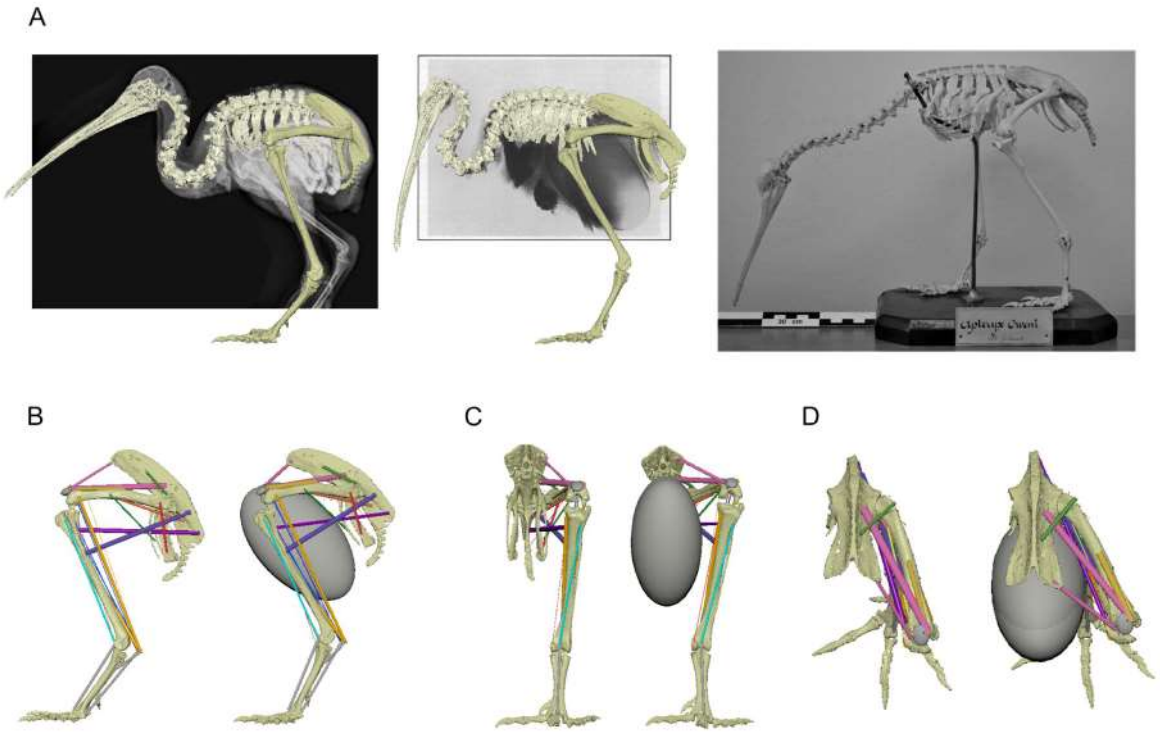

Figure 8

X-ray pictures of the lateral view of a Brown kiwi (*Apteryx mantelli*) (A): bird with no egg on the left and with egg in the middle (modified from Calder, 1979), mounted-skeleton on the right (MNHN 2012-194). Models of the musculoskeletal system of a Brown kiwi (*Apteryx mantelli*) (sternal ribs are missing due to the autopsy) without (on the left) and with an egg (on the right), lateral view (B), frontal view (C), and dorsal view (D).

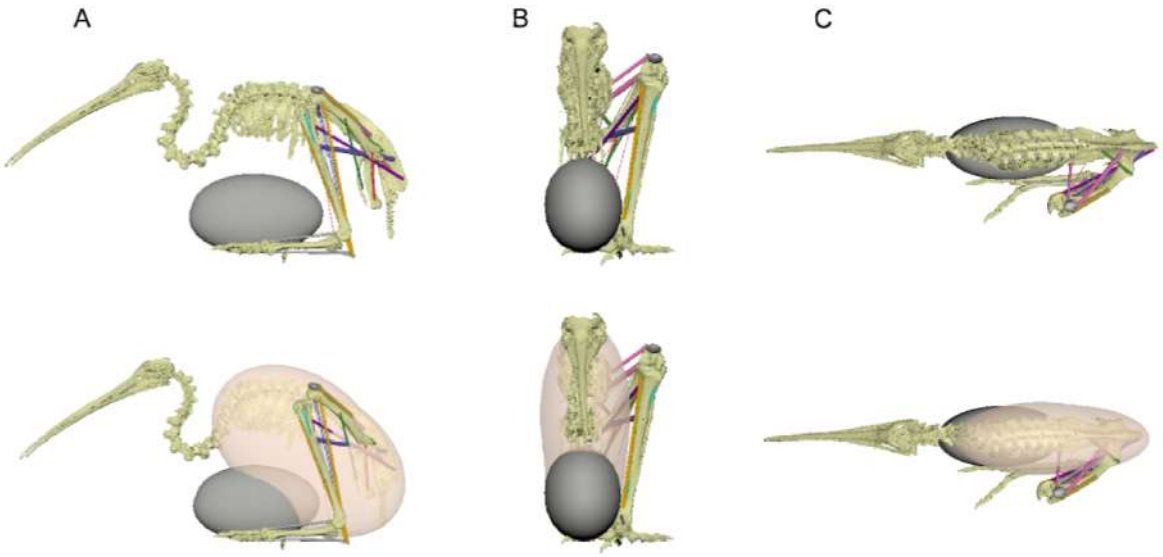

549
550 Figure 9
551 Model of the musculoskeletal system of a brown kiwi (*Apteryx mantelli*) (The sternal ribs are
552 missing due to the autopsy) during brooding on the lateral view (A), frontal view (B), and dorsal
553 view (C). The bottom line shows the position of the body shape during brooding.
554
555
556 **Supplementary material**
557 SM1
558 (A) Table presenting mass and percentage of the total dissected muscle mass of the four
559 dissected specimens. (B) Mass proportion of the kiwi pelvic muscles, compared to ostrich
560 (from Smith et al., 2006) and turkey (Abourachid, 1991). (C)Proportion of the functional
561 groups of muscles in the kiwi the ostrich and the turkey. Ostrich data from Smith (DATE),
562 turkey data from Abourachid (1990). The abbreviations follow the tables 1 and 2 of the present
563 article.

A	A. owenii (male n°55789)		A. owenii (female n°55790)		A mantelli (male n°54765)		A. mantelli (male n°56040)	
	mass (g)	**% total**	**mass**	**% total**	**mass (g)**	**% total**	**mass(g)**	**% total**
Iliotib cran	4.25	6.77%	4.426	5.98%	9.668	6.53%	6.161	5.25%
Iliotib lat	6.51	10.37%	6.725	9.09%	15.48	10.46%	13.641	11.63%
Iliotroch cran	1.04	1.66%	1.07	1.45%	2.048	1.38%	2.038	1.74%
Iliotroch med	0.34	0.54%	0.2	0.27%	0.375	0.25%	0.315	0.27%
Iliotroc cau	4.51	7.19%	4.646	6.28%	10.4	7.02%	6.165	5.26%
Iliofib	5.82	9.28%	5.416	7.32%	14.85	10.03%	11.246	9.59%
Iliofem ext	0.34	0.54%	0.3936	0.53%			0.402	0.34%
Flex cru lat pelv	4	6.37%	4.629	6.25%	8.811	5.95%	9.146	7.80%
Flex cru lat acc	0.29	0.46%	0.312	0.42%	0.853	0.58%	1.162	0.99%
Caudofem cau	0.78	1.24%	0.489	0.66%	1.9	1.28%	1.312	1.12%

Caudofem pelv	3.12	4.97%	3.772	5.10%	8.833	5.97%	6.27	5.34%
Ischiofem	1.21	1.93%	1.217	1.64%				
Obt int	0.18	0.28%	0.318	0.43%				
Amb	0.28	0.44%			0.533	0.36%	0.256	0.22%
Pub isch fem	3.03	4.83%	4.073	5.50%	6.364	4.30%	4.154	3.54%
Femtib lat	5.45	8.69%	7.212	9.74%	15.35	10.37%	8.622	7.35%
Femtib int	1.5	2.38%	1.791	2.42%	2.516	1.70%	2.204	1.88%
Femtibmed	1.37	2.18%	1.663	2.25%	3.169	2.14%	4.589	3.91%
Fib long	2.21	3.52%	2.686	3.63%	4.472	3.02%	3.682	3.14%
Ext dig long	0.89	1.42%	0.9778	1.32%	1.37	0.93%	0.98	0.84%
Tib cran	2.7	4.30%	3.171	4.28%	6.046	4.08%	4.892	4.17%
Gast med	3.87	6.17%	4.693	6.34%	9.854	6.66%	8.871	7.56%
Gast int	0.45	0.71%	0.583	0.79%	1.141	0.77%	1.099	0.94%
Gast lat	2.94	4.68%	3.501	4.73%	8.01	5.41%	6.805	5.80%
Flex ppd II	0.85	1.35%	0.7537	1.02%	0.826	0.56%	1.628	1.39%
Flex ppdiii	0.49	0.77%	1.28	1.73%	2.059	1.39%	0.721	0.61%
Flex pdii	0.73	1.16%	0.786	1.06%	1.9	1.28%	1.398	1.19%
Flex pdiii	1.01	1.61%	1.554	2.10%	1.899	1.28%	1.775	1.51%
Flex pdiv	1.15	1.83%	1.564	2.11%	2.741	1.85%	2.074	1.77%
Fib brev			2.201	2.97%	3.128	2.11%	3.239	2.76%
Flex dig long	1.06	1.69%	1.325	1.79%	1.996	1.35%	1.695	1.44%
Plant	0.4	0.64%	0.58	0.78%	1.46	0.99%	0.772	0.66%
Total	**62.8**		**74.008**		**148.1**		**117.31**	

B

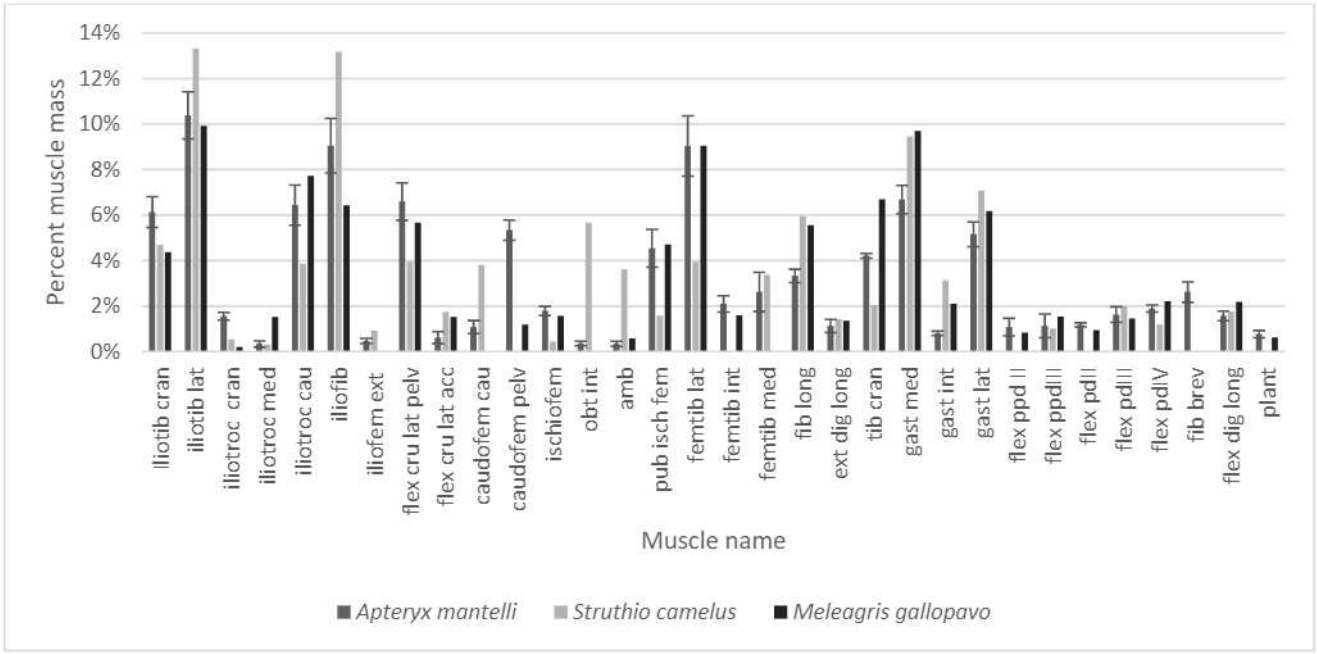

C

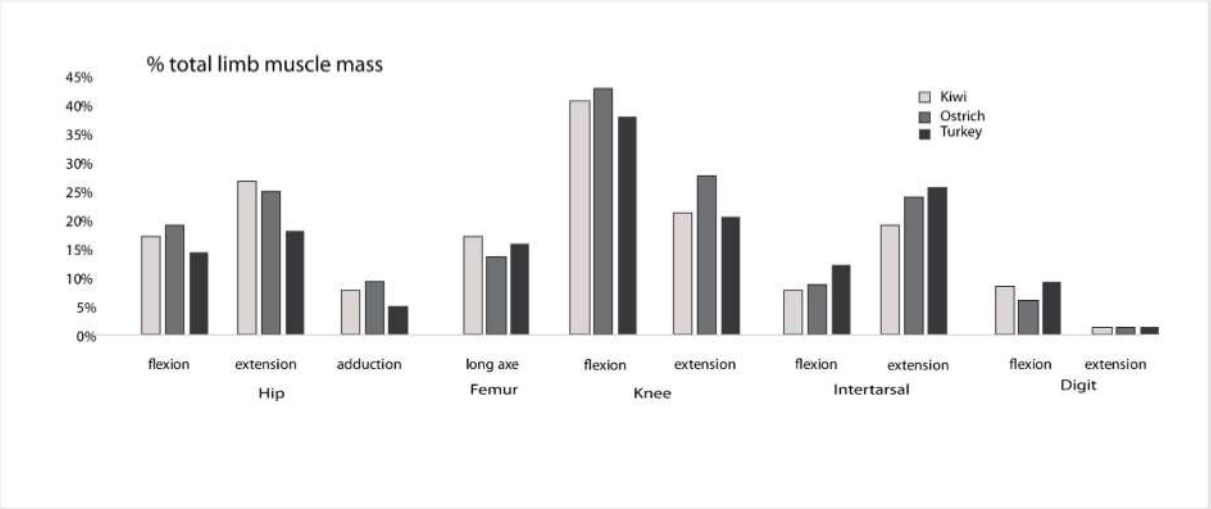

SM2

Video of the 3D models of a standing gravid, non-gravid and incubating kiwi. The associated maya scene is available at https://mycore.core-cloud.net/index.php/f/902116552.

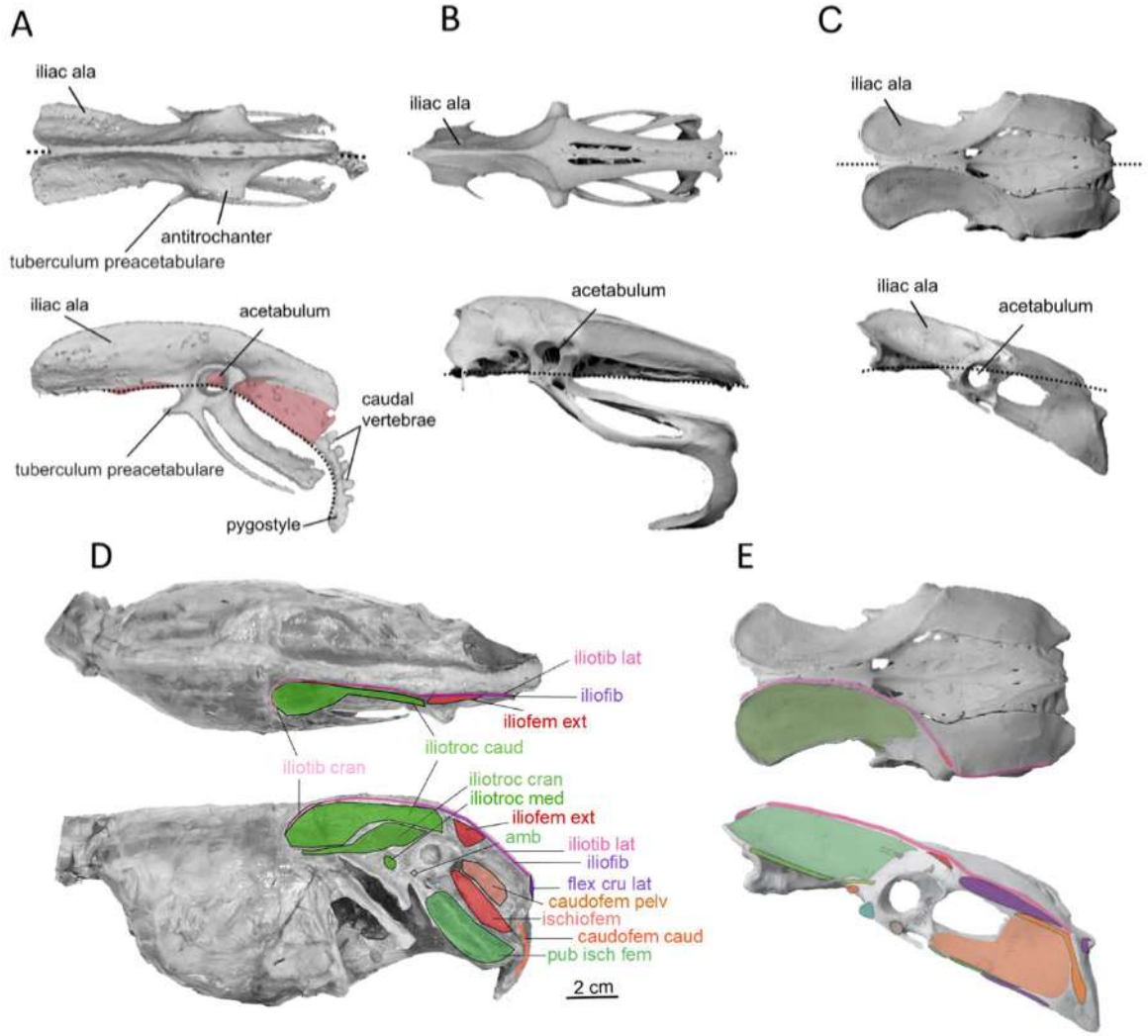

SM3

Osteology of the pelvis of a Brown kiwi (*Apteryx mantelli*) (A), an Ostrich (*Struthio camelus*) (B), and a Turkey (*Meleagris gallopavo*) (C). Dorsal views at the top and lateral views at the bottom, the cranial part points to the left. The dotted line highlights the vertebral column. The synsacrum is highlighted in red on the lateral view of the Brown kiwi.

Muscle origins and insertions on the pelvis of a Brown kiwi (*Apteryx mantelli*) (D) and of a Turkey (*Meleagris gallopavo*) (modified from Abourachid, 1991) (E). Dorsal views at the top, lateral views at the bottom. Abbreviations are following table 1 and table 2.